

## ORIGINAL ARTICLE

# A highly sensitive breathable fuel cell gas sensor with nanocomposite solid electrolyte

Jing Zhang | Gaopeng Jiang | Timothy Cumberland | Pan Xu | Yalin Wu | Stephen Delaat | Aiping Yu | Zhongwei Chen 

Department of Chemical Engineering,  
Waterloo Institute for Nanotechnology,  
Waterloo Institute of Sustainable Energy,  
University of Waterloo, Waterloo, Ontario,  
Canada

## Correspondence

Zhongwei Chen, Department of Chemical Engineering, Waterloo Institute for Nanotechnology, Waterloo Institute of Sustainable Energy, University of Waterloo, 200 University Ave. W., Waterloo, Ontario N2L 3G1, Canada.  
Email: zhwen@uwaterloo.ca

## Funding information

Natural Sciences and Engineering Research Council of Canada; Ontario Centers of Excellence

## Abstract

The present work deals with a poly(vinyl alcohol)-based membrane mixed with poly(4-styrenesulfonic acid) to be used as a proton-conducting solid-state electrolyte in an electrochemical gas sensor for the detection of alcohol. A cross-linking bonding semi-interpenetrating network is formed between the polymer backbones, providing the membrane with superior mechanical property and excellent water retention. Meanwhile, the graphene oxide nanosheets are incorporated into the polymer fibrous backbones, creating impermeable block layers to limit ethanol gas penetration. Importantly, the modification of graphene oxide facilitates the protons transportation in both in-plane and through-plane channels of the membrane, boosting excellent conductivities of  $0.13 \text{ S cm}^{-1}$  (in-plane) and  $22.6 \text{ mS cm}^{-1}$  (through-plane) at  $75^\circ\text{C}$ , respectively. An alcohol fuel cell sensor assembled with this semi-interpenetrating network solid electrolyte membrane is fabricated based on direct ethanol fuel cell principle, exhibiting excellent sensitivity, linearity, as well as low ethanol detection limits of 25 ppm.

## KEYWORDS

electrochemical gas sensor, gel polymer, graphene oxide, proton conductivity, solid electrolyte

## 1 | INTRODUCTION

The global gas sensor market receives a rapid boost during the forecast period owing to ever-increasing demand of gas detections, for example, toxic chemical monitoring in industrial processes, air quality analysis of breathing air, combustible gas detection in vehicles, methane detection in mining applications, as well as measurement of blood alcohol concentration through a breath sample.<sup>1,2</sup> On the basis of different technologies, gas sensors can be divided into various types including catalytic gas sensor, optical gas sensor, semiconductive gas sensor, thermal conductive gas sensor, electrochemical gas sensor, photoionization detector, and so on.<sup>3-5</sup> Among them, electrochemical

gas sensor is regarded as one of the most promising candidates benefitting from its several advantages. First, high sensitivity makes electrochemical gas sensor suitable for low concentration detection in the ppm range.<sup>6,7</sup> Also, the linear relationship between target gas concentration and generated electric current enables electrochemical gas sensor better accuracy and repeatability.<sup>8</sup> Moreover, electrochemical gas sensor usually presents superior selectivity compared to semiconductive and thermal conductive gas sensors, and also has the ability to detect various gases by modifying the materials.<sup>9</sup>

A typical electrochemical gas sensor operates by reacting with the target gas component and outputting electrical signal proportional to gas concentration. The electrode materials of

This is an open access article under the terms of the Creative Commons Attribution License, which permits use, distribution and reproduction in any medium, provided the original work is properly cited.

© 2019 The Authors. *InfoMat* published by John Wiley & Sons Australia, Ltd on behalf of UESTC.

electrochemical gas sensors have key effects on the sensor selectivities through the appointed catalytic reactions with the gases of interest, whereas the electrolyte materials play critical roles in the sensor sensitivities by influencing reaction rate, thereby affecting the outputting electrical signal strength. Therefore, the employment of an excellent electrolyte material is of vital importance for an outstanding electrochemical gas sensor. In general, an ideal electrolyte is supposed to have characteristics of good ionic conductivity as well as excellent thermal and electrochemical stabilities. To date, liquid electrolytes still dominate across the electrochemical gas sensor applications because of their outstanding ionic conductivities benefitting from fast ion mobility and low viscosity.<sup>10-12</sup> However, liquid electrolytes also suffer from leaking problem and drying-out issue after a long period of running, particularly at risk of flammability, volatility, and toxicity if organic solvents are employed in the system. Solid electrolyte membranes could be good alternatives that are simply shaped into multifarious configurations and packages without leaking and drying-out concerns, but the relatively low ionic conductivities largely limit their widely used application. The low ionic conductivity values are because of the ion transportation pathways blocked in the solid-state phase.<sup>13-15</sup> Gel solid electrolytes with unique structures and properties are burgeoning, which create more possibilities to electrolyte development and quickly grab researchers' attention. Gel solid electrolyte is usually composed of a host polymer and a liquid electrolyte or a conductive salt dissolved in a liquid solvent.<sup>16,17</sup> Compared with all-solid-state electrolytes, gel solid electrolytes exhibit superior ionic conductivities because of the presence of liquid phase, which provide a freer and easier moving pathway for ions rather than the blocked all-solid-state phase.<sup>18</sup> Moreover, the host polymer can serve as the three-dimensional network to trap the liquid phase into the polymer matrix, giving the membrane a robust and flexible solid framework. However, because of the fibrous three-dimensional network structure, the gel solid electrolytes are unable to block the gas molecules flowing through their inner porous channels, which limits their applications as solid electrolytes in electrochemical gas sensors. Graphene oxide (GO), the oxidation product of natural graphite flakes, is widely used as chemical or thermal modified material. Importantly, the abundant carboxylic acid groups on the edges of GO sheets impart negative charges when exfoliated in water,<sup>19,20</sup> and these negatively charged nanosheets are impermeable to most gases, such as methanol, ethanol, methane and carbon dioxide, thus making it promising candidate as gas barrier nanocomposite.<sup>21-23</sup>

## 2 | RESULTS AND DISCUSSIONS

In this present work, taking the advantages of high ionic conductivity from gel solid electrolytes and gas barrier

characteristic from GO nanosheets, a proton-conducting semi-interpenetrating network solid electrolyte was designed and applied in an electrochemical gas sensor on the basis of fuel cell technology for the detection of ethanol, namely alcohol fuel cell sensor. As shown in Figure 1, first, poly(vinyl alcohol) (PVA) is employed as host polymer matrix mixed with poly(4-styrenesulfonic acid) (PSSA), followed by adding of GO into this system to obtain uniform hydrogel solution. Second, the blended hydrogel solutions are then casted into membranes at room temperature by drying-out of free water molecules. PVA is the most popular hydrogel polymer host that contains carbon chain backbone with hydroxyl groups attached to methane carbons. The abundant OH groups can assist the PVA-based complex in the formation of a polymer-blended membrane through hydrogen bonding. The PVA-based membranes can also be endowed with proton-conducting ability in the presence of acid polymer PSSA. Together with low ethanol permeability of GO, the PVA-PSSA-GO membranes are obtained and could be ideal candidate materials in ethanol gas sensor applications. However, hydrophilic property of PVA membrane makes it usually suffering from bad-dimensional stability and high-swelling degree. Therefore, the last procedure, chemical crosslinking, is essential for giving the PVA-based membranes more stable structure. Glutaraldehyde is applied as cross-linker in this work to chemically cross-link the hydroxyl groups of PVA with acetal ring, making a dense and regular semi-interpenetrating network that can successfully trap acid PSSA polymer and GO into the membrane backbones. After all of these blending, casting, and cross-linking procedures, a proton-conducting semi-interpenetrating network solid electrolyte is obtained in the application of an electrochemical gas sensor for the detection of alcohol.

Proton-conducting level is a key evaluation criterion for an electrolyte membrane. Some electrolyte membranes exhibit morphological anisotropy based on different membrane casting methods or membrane pretreatment procedure. These membranes' morphological anisotropies could lead to anisotropic ionic conductivities that can be separated into in-plane conductivity and through-plane conductivity. Most reported literature values are based on the ion transportations measure along the plane of membranes, that is, in-plane conductivity.<sup>24,25</sup> However, through-plane conductivity is much more practical for most electrochemical applications, in which proton transportation is perpendicular to membranes.<sup>26</sup> Therefore, it is inaccurate to evaluate membrane's proton-conducting ability individually relying on in-plane or through-plane conductivity. Particularly, special ion transportation pathways may form because of the employment of specific two-dimensional GO nanosheets. In this work, in order to fully understand the in-plane and through-plane conductivities for this polymer composite system, the PVA-PSSA-GO membranes are prepared by mixing

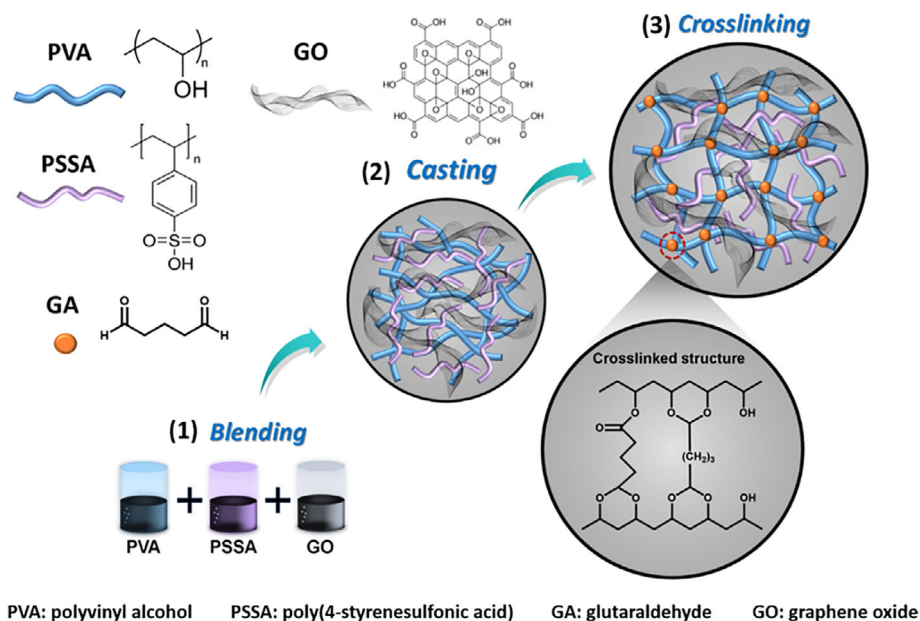


**FIGURE 1** Materials and synthetic procedure of PVA-PSSA based solid membrane with GO modification

of different PSSA and GO contents into PVA matrix. As shown in Figure 2A,C, both in-plane and through-plane conductivity values of membranes increased with the increasing contents of PSSA, resulting in outstanding conductivity values of 58.0 and 21.3  $\text{mS cm}^{-1}$  for in-plane and through-plane, respectively. That is because more PSSA inside the system could provide more proton conducting sites. Figure 2B,D exhibit the in-plane and through-plane conductivities of membranes prepared by mixing of 1%, 3%, 5%, and 7% weight percentage of GO into with polymer composition of 1:0.5 (PVA:PSSA) by mass as a typical candidate. More GO contents induce larger in-plane conductivity values from 37.6 (1%) to 54.4  $\text{mS cm}^{-1}$  (7%), indicating that GO additives facilitate the movement of protons along the plane of membranes. More GO nanosheets could form more layered ion transportation channels along the polymer matrix inner structure.<sup>27</sup> However, these two-dimensional GO nanosheets also block the pathway of ions to pass across the direction of the thickness of membranes, which results in a gradual descending trend from 12.9 (1%) to 10.2  $\text{mS cm}^{-1}$  (7%) for through-plane conductivity. The anisotropy values of membranes are calculated to further investigate the proton transportations. As shown in Figure 2E, without the addition of GO, the PVA-PSSA polymer membranes exhibit a slightly decreasing of anisotropy values from 4.4 to 2.7. That is because more PSSA contents could provide more proton-conducting sites, which will weaken the anisotropic ion conductive phenomenon. However, as shown in Figure 2F, after the addition of GO, the membranes show gradually increasing anisotropy values from 2.9 to 5.3, indicating that more GO nanosheets could create more in-plane proton transportation

channels as well as more block impermeable layers that limit the proton transportation across the membranes.<sup>28</sup>

The temperature dependencies of proton conductivities are also investigated to further investigate the ion transportation mechanism. As shown in Figure 3A,B, both in-plane and through-plane conductivities of PVA-PSSA by the mass of 1:0.5 exhibit growing proton conductive values with the increasing temperature, finally achieve impressive proton conductive values of 0.13  $\text{S cm}^{-1}$  (in-plane) and 22.6  $\text{mS cm}^{-1}$  (through-plane) at 75°C, respectively. Similarly, after addition of GO into the system, the PVA-PSSA-GO polymer membranes also show positive temperature-conductivity linear relationship. In Figure 3C,D, the activation energies are calculated on the basis of the Arrhenius equation, achieving data of 15.38 and 11.92 (5% GO)  $\text{kJ mol}^{-1}$  for in-plane, and 7.88 and 9.21 (5% GO)  $\text{kJ mol}^{-1}$  for through-plane, respectively. According to the activation energy values, two ion transportation mechanisms, that is, vehicle and Grotthuss mechanisms, occur simultaneously in this complex system. In the presence of abundant water molecules, protons are tended to be dissociated from the sulfuric acid groups, and then form into hydrated  $\text{H}_3\text{O}^+$  ions with surrounding water molecules.<sup>29-31</sup> The hydrated  $\text{H}_3\text{O}^+$  ions then migrate along the GO in-plane nanochannels according to the ion concentration gradient, which is also defined as vehicle mechanism. Compared with vehicle mechanism, Grotthuss mechanism requires lower activation energy, in which the protons transport through hopping between two neighbor conducting sites without any carrier molecules.

The performance of PVA-PSSA-GO membrane is evaluated in an ethanol gas sensor. The membrane electrode assembly (MEA) is the core component of sensor composed of the

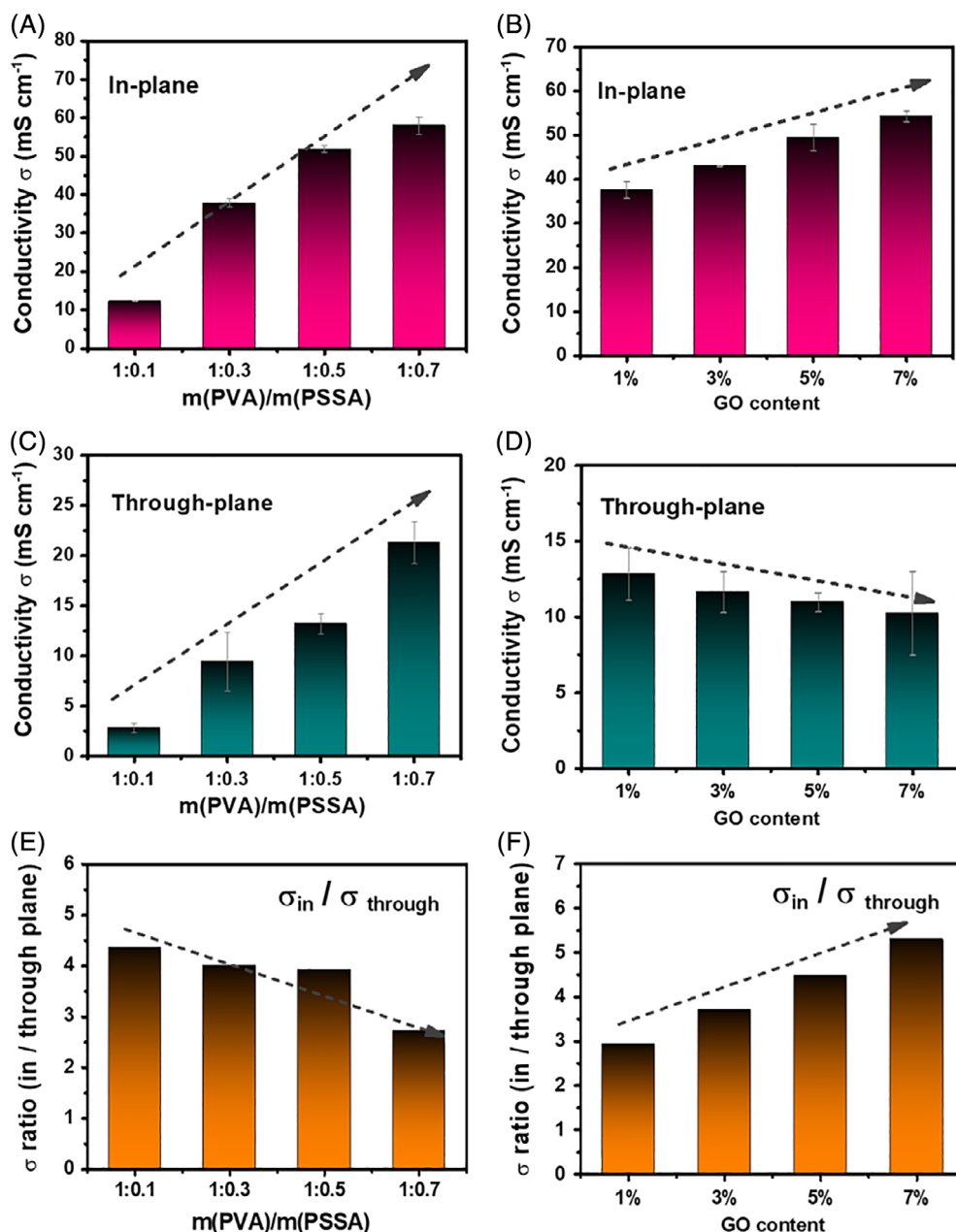


**FIGURE 2** A and C, In-plane and through-plane proton conductivity of PVA-based membrane with different PSSA contents. B and D, In-plane and through-plane proton conductivity of PVA-PSSA membrane with the addition of different GO contents. E and F, Anisotropic conductivity values of PVA-based membrane with different PSSA and GO contents (PVA-PSSA by the mass of 1:0.5 as a typical candidate for all GO addition)

PVA-PSSA-GO membranes and two commercial gas diffusion electrodes (GDEs). The PVA-PSSA-GO membrane is sandwiched between two electrodes with Pt/C catalyst coated on both anode and cathode. As shown in Figure S5, the sensor performance is investigated in a system consisting of sensor as well as alcohol simulator, flow meter, moisture separator, data recorder, and computer analyzer. An alcohol simulator is applied for the purpose of humidity/temperature simulation of human breath. When a quantified air is pumped through the alcohol simulator, a certain concentration of ethanol vapor is brought out with the air. As shown in Figure 4A,

the ethanol oxidation reaction (EOR) occurs immediately as long as the ethanol vapor diffuses into the anode, generating protons and electrons. Protons transport across the PVA-PSSA-GO electrolyte membrane and react with oxygen at the cathode, triggering oxygen reduction reaction (ORR) and producing water. Electrons travelling from external circuit are collected as electrical signals that exhibit positive linear relationship with the concentration of input ethanol vapor. By analyzing the electrical signals in computer analyzer, a typical response current curve is obtained with characterizations of four different parameters: peak height, peak area, response

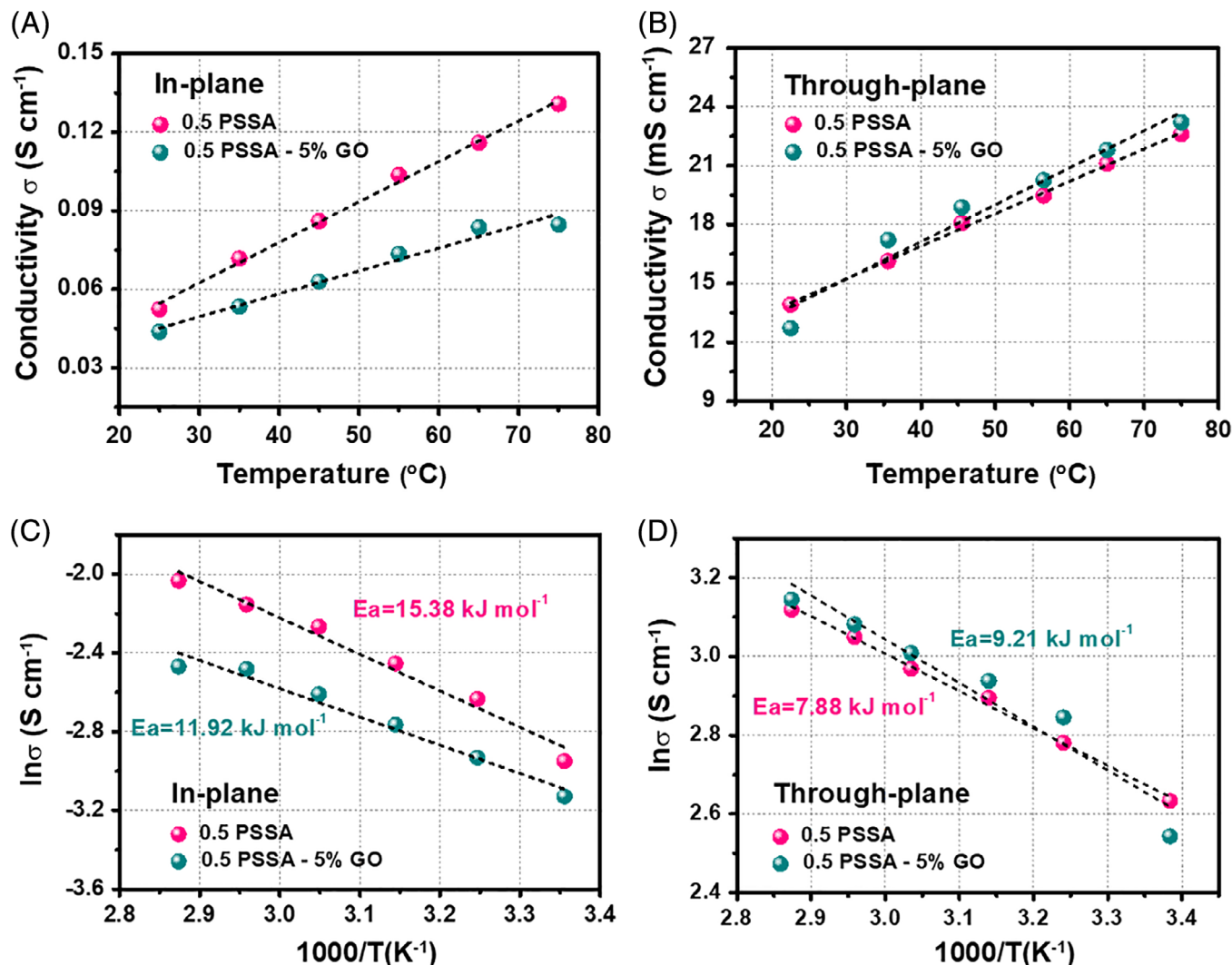


**FIGURE 3** A and B, In-plane and through-plane proton conductivities. C and D, Arrhenius plot of in-plane and through-plane proton conductivity of PVA-PSSA membrane by mass of 1:0.5, and the addition of 5% GO contents as a function of temperature

time, and recovery time. In theory, the ethanol concentration exhibits a linear relationship with peak area corresponding to the quantity of transferred electrons. Accordingly, the ethanol concentration can be calculated by Equation (1)

$$c = \frac{A_{peak}}{nFV} \quad (1)$$

where  $c$  refers to the ethanol concentration in vapor,  $n$  is corresponding to the number of transferred electrons in the reaction,  $V$  is the volume of ethanol vapor into the sensor,  $A_{peak}$  is the peak area, and  $F$  is the Faraday constant.

In Figure 4B, the performance of sensors fabricated from PVA-PSSA polymer membranes with different PSSA contents are investigated in ethanol solution, which is prepared equivalent to blood alcohol concentration (BAC) of 50 mg dL<sup>-1</sup>. Evidently, the PVA-PSSA membrane with the mass ratio

of 1:0.7 has the biggest peak area and peak height among all the four membranes. That is because more proton conducting sites can easier conduct protons, resulting in superior response to ethanol. In Figure 4C, after the addition of 5% GO, the membrane exhibits similar response curve but with a larger peak area. Because without the addition of GO nanosheets, the residual ethanol vapor may pass across the PVA-PSSA membrane owing to its fibrous polymer structure, finally causing the gas permeates problem. However, after adding of GO nanosheets that has low permeability to ethanol gas, the sensor exhibits larger peak area due to its resistance to ethanol vapor mass transfer. Additionally, as shown in Figure 4D, the peak areas of PVA-PSSA-GO membrane based sensors are also calculated on the basis of different concentrations of ethanol solutions, which show excellent linearity with the detection limit to 25 ppm in human breath, corresponding to an ethanol solution that is

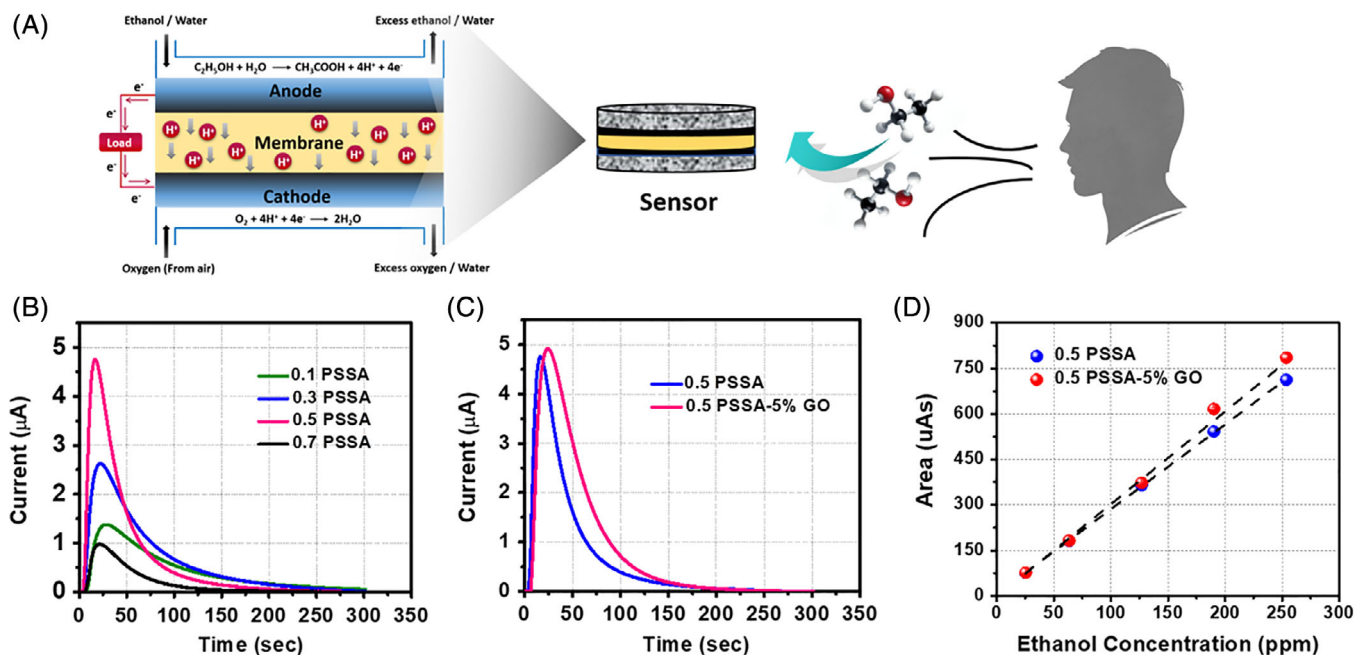


**FIGURE 4** A, Schematic diagram of an ethanol fuel cell sensor and its electrochemical principle. B, Response curves of sensors employing PVA-based membranes with different PSSA contents. C, Response curves of sensors employing PVA-PSSA membrane by the mass of 1:0.5 before and after 5% GO addition. D, The peak areas obtained from response curves vs ethanol concentration in the vapor

equivalent to BAC as low as  $10 \text{ mg dL}^{-1}$ . The sensor sensitivity is as investigated as the fitted slope of linearity curves. As shown in Figure 4D, both of them exhibit excellent linear relationships between the curve areas and the ethanol concentrations with the linear regressions  $R^2$  values of .99975 and .99151. These values represent how much the curve areas change as a response to changes in the ethanol concentrations. Thus, the PVA-PSSA membrane is as sensitive as PVA-PSSA-GO membrane for the detection of ethanol.

### 3 | CONCLUSION

In conclusion, PVA/PSSA-based membranes with the modification of GO are designed and fabricated as proton-conducting solid-electrolyte membranes. Cross-linking technique is successfully applied in this system to provide a tough and robust semi-interpenetrating skeleton with superior mechanical property and excellent water retention. An electrochemical gas sensor on the basis of fuel cell technology is demonstrated with the membrane for the detection of alcohol, exhibiting excellent sensitivity, great linearity, as well as low ethanol detection limits to 25 ppm. Meanwhile, the graphene oxide nanosheets are incorporated into the polymer fibrous backbones, creating impermeable block layers to limit ethanol gas penetration. Importantly, the modification of GO facilitates the protons transportation in both in-plane and through-plane channels of the membrane,

boosting excellent conductivities of  $0.13 \text{ S cm}^{-1}$  (in-plane) and  $22.6 \text{ mS cm}^{-1}$  (through-plane) at  $75^\circ\text{C}$ , respectively.

### 4 | EXPERIMENTAL SECTION

**Synthesis of GO:** GO was synthesized from natural graphite flakes on the basis of the improved Hummers' method. First, concentrated  $H_3PO_4$  (40 mL, 85%) and  $H_2SO_4$  (360 mL, 98%) were carefully blended in an ice-bath conditioned flask. Graphite powder (2 g) was slowly added into the mixed solution and continually stirred for 1 h. Afterward,  $KMnO_4$  (18 g) was added into the mixture as strong oxidizing agent, leading to the oxidation reaction kept at  $50^\circ\text{C}$  for 16 h. The oxidation reaction was terminated after cooling down the mixture.  $H_2O_2$  (20 mL, 30%) and distilled deionized (DDI) water (400 mL) were added dropwise into the mixture and then stirred for 30 min. Last, the mixed solution was centrifuged and washed with DDI water, HCl (5%), and ethanol, respectively. The final GO nanosheets were obtained by freeze-drying.

**Fabrication of PVA-PSSA-GO membrane:** The PVA-PSSA-GO membranes were prepared by a simple solution-casting method. A PVA (99% hydrolyzed, Mw: 86000-89 000, Aldrich) solution was obtained by dissolving PVA (50 g) in distilled water (500 mL). The PVA solution was heated at  $90^\circ\text{C}$  and continuously stirred until a uniform and transparent solution was obtained. PSSA (18 wt.% Mw  $\sim 75$  000,

Aldrich) was then mixed with the above PVA solution in selected blend ratios: PVA/PSSA being 1:0.1, 1:0.3, 1:0.5, 1:0.7 by mass. After that, PVA/PSSA by the mass of 1:0.5 was chosen as a typical sample with an addition of different GO contents of 1%, 3%, 5%, 7% by mass. Then the resulting solutions were poured into plastic Petri dishes. After drying out the water, the membrane was peeled from the plastic substrate. Chemical cross-linking process was proceeded by soaking the membranes in reaction solution consisting of 10 wt.% glutaraldehyde, 0.2 wt.% hydrochloric acid in acetone for 2 h. Last, the membranes were taken out and rinsed repeatedly with deionized water for final measurements.

**Electrochemical gas sensor evaluation:** The gas sensor performance was evaluated on the basis of fuel cell technology. First, MEAs were prepared with a series of PVA-PSSA-GO membranes sandwiched between commercial GDE (Fuelcell Etc.). Sixty percent Pt/C catalysts with a Pt loading of  $0.5 \text{ mg cm}^{-2}$  were coated on both anode and cathode. Afterward, the sensor housing was assembled with the MEA composed of the as-prepared membrane and two electrodes. Then, the sensor housing should equilibrate the components in the humidity chamber (BTL-433) with  $25^\circ\text{C}$  and RH 60% for 72 h to reach the desired condition. The resulting sensor performance was then evaluated by inserting the sensor housing into the testing. Each sample was repeated five times within a 30-minute testing period and the average of was parameter was taken into account.

## ACKNOWLEDGMENTS

This work was financially supported by the Natural Sciences and Engineering Research Council of Canada (NSERC), and Ontario Centers of Excellence (OCE). All the financial supports are gratefully acknowledged.

## CONFLICT OF INTEREST

The authors declare no conflict of interest.

## ORCID

Zhongwei Chen  <https://orcid.org/0000-0003-3463-5509>

## REFERENCES

1. Zheng ZQ, Yao JD, Wang B, Yang GW. Light-controlling, flexible and transparent ethanol gas sensor based on ZnO nanoparticles for wearable devices. *Sci Rep*. 2015;5:11070.
2. Zhang J, Liu X, Neri G, Pinna N. Nanostructured materials for room-temperature gas sensors. *Adv Mater*. 2016;28:795-831.
3. Hagleitner C, Hierlemann A, Lange D, et al. Smart single-chip gas sensor microsystem. *Nature*. 2001;414:293-296.
4. Modi A, Koratkar N, Lass E, Wei B, Ajayan PM. Miniaturized gas ionization sensors using carbon nanotubes. *Nature*. 2003;424:171-174.
5. Kalantar-zadeh K, Ou JZ, Daeneke T, Mitchell A, Sasaki T, Fuhrer MS. Two dimensional and layered transition metal oxides. *Appl Mater Today*. 2016;5:73-89.
6. Park C, Fergus J, Miura N, Park J, Choi A. Solid-state electrochemical gas sensors. *Ionics*. 2009;15:261-284.
7. Stetter JR, Penrose WR, Yao S. Sensors, chemical sensors, electrochemical sensors, and ECS. *J Electrochem Soc*. 2003;150:S11-S16.
8. Jiang G, Goledzinowski M, Comeau FJ, et al. Free-standing functionalized graphene oxide solid electrolytes in electrochemical gas sensors. *Adv Funct Mater*. 2016;26:1729-1736.
9. Fine G, Cavanagh L, Afonja A, Binions R. Metal oxide semiconductor gas sensors in environmental monitoring. *Sensors*. 2010;10:5469-5502.
10. Li W, Dahn JR, Wainwright DS. Rechargeable lithium batteries with aqueous electrolytes. *Science*. 1994;264:1115-1118.
11. Huang WS, Humphrey BD, MacDiarmid AG. Polyaniline, a novel conducting polymer: morphology and chemistry of its oxidation and reduction in aqueous electrolytes. *J Chem Soc, Faraday Trans 1*. 1986;82:2385-2400.
12. Beck F, Rüetschi P. Rechargeable batteries with aqueous electrolytes. *Electrochim Acta*. 2000;45:2467-2482.
13. Armand M. Polymer solid electrolytes-an overview. *Solid State Ion*. 1983;9:745-754.
14. Bruce PG. *Solid State Electrochem*. Cambridge, United Kingdom: Cambridge University Press; 1997.
15. Hagenmuller P, Van Gool W. *Solid Electrolytes: General Principles, Characterization, Materials, Applications*. New York: Elsevier; 2015.
16. Stephan AM. Review on gel polymer electrolytes for lithium batteries. *Eur Polym J*. 2006;42:21-42.
17. Meyer WH. Polymer electrolytes for lithium-ion batteries. *Adv Mater*. 1998;10:439-448.
18. Song J, Wang Y, Wan CC. Review of gel-type polymer electrolytes for lithium-ion batteries. *J Power Sources*. 1999;77:183-197.
19. Berean KJ, Ou JZ, Daeneke T, et al. 2D MoS<sub>2</sub>/PDMS nanocomposites for NO<sub>2</sub> separation. *Small*. 2015;11:5035-5040.
20. Berean KJ, Ou JZ, Nour M, et al. Enhanced gas permeation through graphene nanocomposites. *J Phys Chem C*. 2015;119:13700-13712.
21. Kumar R, Mamlouk M, Scott K. A graphite oxide paper polymer electrolyte for direct methanol fuel cells. *Int J Electrochem*. 2011;2011:1-12.
22. Nair RR, Wu HA, Jayaram PN, Grigorieva IV, Geim AK. Unimpeded permeation of water through helium-leak-tight graphene-based membranes. *Science*. 2012;335:442-444.
23. Joshi RK, Carbone P, Wang FC, et al. Precise and ultrafast molecular sieving through graphene oxide membranes. *Science*. 2014;343:752-754.
24. Soboleva T, Xie Z, Shi Z, Tsang E, Navessin T, Holdcroft S. Investigation of the through-plane impedance technique for evaluation of anisotropy of proton conducting polymer membranes. *J Electroanal Chem*. 2008;622:145-152.
25. Argun AA, Ashcraft JN, Hammond PT. Highly conductive, methanol resistant polyelectrolyte multilayers. *Adv Mater*. 2008;20:1539-1543.
26. Li J, Park JK, Moore RB, Madsen LA. Linear coupling of alignment with transport in a polymer electrolyte membrane. *Nat Mater*. 2011;10:507-511.

27. Karim MR, Hatakeyama K, Matsui T, et al. Graphene oxide nanosheet with high proton conductivity. *J Am Chem Soc.* 2013; 135:8097-8100.
28. Hatakeyama K, Karim MR, Ogata C, et al. Proton conductivities of graphene oxide nanosheets: single, multilayer, and modified nanosheets. *Angew Chem Int Ed.* 2014;53:6997-7000.
29. Kreuer K-D, Rabenau A, Weppner W. Vehicle mechanism, a new model for the interpretation of the conductivity of fast proton conductors. *Angew Chem Int Ed.* 1982;21:208-209.
30. Day TJJ, Schmitt UW, Voth GA. The mechanism of hydrated proton transport in water. *J Am Chem Soc.* 2000;122:12027-12028.
31. Marx D, Tuckerman ME, Hutter J, Parrinello M. The nature of the hydrated excess proton in water. *Nature.* 1999;397:601-604.

## SUPPORTING INFORMATION

Additional supporting information may be found online in the Supporting Information section at the end of this article.

**How to cite this article:** Zhang J, Jiang G, Cumberland T, et al. A highly sensitive breathable fuel cell gas sensor with nanocomposite solid electrolyte. *InfoMat.* 2019;1:234–241. <https://doi.org/10.1002/inf2.12017>